CHEMICAL ENGINEERING TRANSACTIONS

VOL. 122, 2025

A publication of AIDIC

The Italian Association of Chemical Engineering
Online at www.cetjournal.it

Guest Editors: Jeng Shiun Lim, Bohong Wang, Guo Ren Mong, Petar S. Varbanov

ISBN 979-12-81206-23-6; **ISSN** 2283-9216

DOI: 10.3303/CET25122041

Flame Spray Pyrolysis Synthesis of NiFe/TiO_2 for Catalytic Deoxygenation in Biojet Fuel Production

Jianxin Zhang[a], Brandon Han Hoe Goh[a], Jo-Han Ng[b], Cheng Tung Chong[a,*]

[a]China-UK Low Carbon College, Shanghai Jiao Tong University, Lingang, Shanghai 201306, China
[b]Carbon Neutrality Research Group, University of Southampton Malaysia, 79100 Iskandar Puteri, Johor, Malaysia
ctchong@sjtu.edu.cn

Flame spray pyrolysis (FSP) was employed to synthesize a novel NiFe bimetallic catalyst with enhanced deoxygenation performance for biojet fuel production. The FSP method enables the rapid, one-step formation of bimetallic catalyst with uniform metal dispersion and controlled nanostructure. Catalytic deoxygenation was performed on trimethylolpropane trioleate (TMPTO) under nitrogen atmosphere at ambient pressure, targeting hydrocarbon products in the C8-C16 range. Comparative analysis with conventionally impregnated catalysts was done to assess the advantages of FSP in tailoring catalyst structure, improving metal dispersion and enhancing deoxygenation activity. This work provides a promising synthesis method for developing a rapid catalyst production system for biojet fuel production and lays the groundwork for the development of other FSP-synthesized bimetallic catalysts.

1. Introduction

With the increasing demand for biojet fuels and the urgent need to reduce carbon emissions, the catalytic upgrading of waste lipid feedstocks into hydrocarbon fuels has garnered significant attention as a viable route toward circular carbon economy. Catalytic deoxygenation is an important route for the conversion of waste lipid feedstocks into valuable liquid fuels, where triglycerides can be cracked, deoxygenated and isomerized into the suitable hydrocarbons. The reaction process typically follows a two-step pathway, consisting of deoxygenation to remove oxygenated functional groups, followed by isomerization to improve fuel properties (Goh et al., 2024). To enhance process efficiency and reduce operational complexity, recent research has increasingly focused on developing single-step multifunctional catalysts capable of coupling deoxygenation, cracking, and isomerization in one reactor. Recently, catalysts synthesized from noble metals such as Pt, Pd, Ru (Wu & Cai, 2022) or non-precious metals such as Fe, Co, Ni (Romero et al., 2022) loaded on solid acid supports has been suggested to enable the conversion of waste lipid feedstocks into biojet fuels through simultaneous deoxygenation, cracking and isomerization. Hartati et al. (2025) synthesized trifunctional Ni/Ca/ZSM-5 catalysts from volcanic mud and marble waste in waste oil and grease, which exhibited 66.6 % C15-C17 selectivity in their results. The acidic properties of elemental Ni showed significant selectivity for long-chain hydrocarbons. Tang et al. (2023) synthesized a Ni_x-Fe/SAPO-11 catalyst for solvent-free hydrodeoxygenation (HDO) in jatropha oil with 15 bar H_2 pressure. The results showed excellent cyclization and deoxygenation activities, with yields of 12.03 % for cycloalkanes, 59.83 % for straight-chain alkanes, and 55.04 % for hydrocarbons in the C8-C16 range. One-step HDO and cleavage isomerization by the synergistic action of metal elements on acidic carriers. Çakan et al. (2023) investigated the catalytic HDO of safflower oil, a feedstock primarily composed of oleic acid (37.85 %), linoleic acid (44.62 %), palmitic acid (7.41 %), and linolenic acid (5.60 %). In their study, cobalt was selected as the active metal, supported on four different carriers: γ-Al_2O_3, TiO_2, ZnO, and ZrO_2. The results demonstrated that the 10 wt% Co/ZnO catalyst exhibited superior performance under optimized reaction conditions (350 °C 8 h, 7.5 MPa), achieving a notable C9-C16 hydrocarbon selectivity of 65.96 %. The metallic component exhibits a hydrogenolytic effect, significantly facilitating hydrogen dissociation and thereby promoting the deoxygenation kinetics. Meanwhile, the acidic carrier plays a crucial role in cleaving and isomerizing long-chain alkanes, effectively converting them into the desired C8-C16 hydrocarbon products. However, despite these advances, several critical gaps remain. Most catalytic processes still depend on high-pressure hydrogenation, raising

Paper Received: 3 September 2025; Revised: 17 October 2025; Accepted: 3 December 2025
Please cite this article as: Zhang J., Goh B.H.H., Ng J.-H., Chong C.T., 2025, Flame Spray Pyrolysis Synthesis of NiFe/TiO2 for Catalytic Deoxygenation in Biojet Fuel Production, Chemical Engineering Transactions, 122, 241-246 DOI:10.3303/CET25122041

concerns regarding safety, economic feasibility, and the need for complex hydrogen infrastructure. Additionally, issues such as catalyst stability, selectivity control, and adaptation to diverse lipid feedstock compositions require further research to achieve scalable and robust biojet production pathways.

Conventional catalyst synthesis methods such as wet impregnation often suffer from poor metal dispersion, weak metal-support interaction, and lack of structural tunability, resulting in limited long-term stability under harsh reaction conditions. Flame spray pyrolysis (FSP) is a versatile and scalable technique for synthesizing metal oxide nanoparticles, offering notable advantages such as operational simplicity, rapid single-step processing, and precise control over particle morphology and composition (Zhang et al., 2024a) . The ultra-high flame temperature (~1,500–2,000 °C), coupled with rapid quenching, facilitates the formation of nanoscale particles with uniform dispersion and a high density of surface-active sites. This process also enhances metal–support interaction and suppresses sintering, contributing to long-term catalytic stability. Moreover, the in-situ calcination in the high-temperature flame endows the resulting metal oxide particles with excellent crystallinity and thermal stability (Minegishi et al., 2024). Lei et al. (2025). demonstrated that the Y/Al atomic ratio critically controls the morphology of flame-synthesized Y-Al nanoparticles, with higher ratios promoting spherical particle formation and subsequent aggregation due to increased melting points. Wei et al. (2024) prepared 2 wt% Fe-doped TiO_2 nanoparticles, where the lattice doping induced rutile phase transformation and oxygen defect formation, enhancing radical trapping capability in silicone rubber matrices. The method's adaptability extends to multicomponent systems, where in-situ calcination ensures strong metal-support interactions, mitigating deactivation in harsh environments. Compared to conventional methods such as wet impregnation (WI) or sol–gel synthesis, FSP has been shown to yield smaller particle size (<10 nm), higher BET surface area, and stronger metal–support interaction due to rapid nucleation. These features are particularly advantageous for multicomponent catalyst systems, including bimetallic or doped structures, where FSP enables atomic-level dispersion and synergistic electronic effects. Recent studies have shown that FSP-synthesized bimetallic catalysts exhibit enhanced activity and stability in harsh reaction environments due to robust interfacial bonding and defect engineering. Thus, FSP provides the option for rational design of nanostructured catalysts tailored for high-performance applications. Currently, there is a lack of study in examining the potential of FSP-synthesized bimetallic catalysts under hydrogen-free conditions for the selective production of jet fuel range-hydrocarbons. While FSP has been proven effective for producing stable and dispersed metal oxides, its application to design bifunctional catalysts capable of promoting both deoxygenation and skeletal rearrangement in waste lipid upgrading remains underexplored.

In this study, NiFe/TiO_2 catalysts are synthesized by FSP method to investigate the synergistic interaction between Ni and Fe and how the preparation method affects the catalytic performance. The selectivity of NiFe/TiO_2 for hydrocarbons in the C8-C16 range under N_2 atmosphere is analysed. In order to synthesise a bifunctional catalyst that promotes both deoxygenation and isomerization, TiO_2 with acidity is chosen as the support to provide both metal dispersion and acidic functionality. Trimethylolpropane trioleate (TMPTO), a typical long-chain oxygenated compound, was employed as a model reactant to assess the catalyst's deoxygenation capability under an inert atmosphere. This work aims to comprehensively investigate the structural and physicochemical characteristics of the bimetallic catalyst produced via flame spray pyrolysis and reveal the correlations between catalyst structure and performance.

2. Materials and Methods

2.1 Catalyst preparation

The catalysts were synthesized via flame spray pyrolysis method. For comparison, catalysts prepared by conventional wet impregnation were used as a control to evaluate the performance of FSP-derived samples. For the conventional wet impregnation (WI) method, aqueous solutions of nickel and iron nitrate hexahydrates (total metal loading: 2 g, molar ratio 1:1) were stirred in 10 mL deionized water. A homogeneous mixture was formed by ultrasonication and impregnated with 10 g of TiO_2 support. After overnight drying (100 °C for 12 h), the material was calcined in a tubular furnace under N_2 flow (250 mL/min) at 550°C (10°C/min) for 4 h, yielding the NiFe/TiO_2 catalyst (Zhang et al., 2024b), herein denoted as NiFe/TiO_2 (WI).

For the FSP method, the NiFe/TiO_2 catalysts were synthesized using an in-house developed FSP system as shown in Figure 1. First, 50 mL of 0.5 M ethanolic solution of $Fe(NO_3)_3 \cdot 9H_2O$ and $Ni(NO_3)_2 \cdot 6H_2O$ (1:1 molar ratio) was atomized at 3.5 mL/min using compressed air (11 L/min) through a custom-designed co-flow nozzle. Heat was provided by the combusted CH_4 premixed with air at 0.65 L/min and 7.5 L/min, respectively. The nanoparticles were collected on a stainless-steel mesh (1000 mesh, pore size 16 μm) via vacuum-assisted deposition (-10 kPa) downstream of the flame quenching zone, producing the NiFe/TiO_2 catalyst, denoted as NiFe/TiO_2 (FSP).

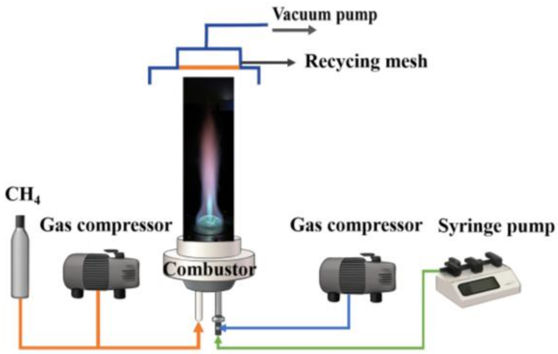

Figure 1: Schematic of FSP system

2.2 Catalyst characterization

The physicochemical properties of the synthesized catalysts were comprehensively characterized using multiple analytical techniques. Morphological features and elemental compositions were investigated by scanning electron microscopy (SEM, ZEISS Gemini 300) coupled with energy-dispersive X-ray spectroscopy (EDS, Oxford X-MaxN 80) at 15 kV acceleration voltage. Crystal structure analysis was performed by X-ray diffraction (XRD, Bruker D8 Advance) using Cu-Kα radiation (λ = 1.5406 Å) with a scanning range of 5-90° (2θ) at 2°/min. Textural properties including specific surface area, pore volume and pore size distribution were determined through N_2 physisorption measurements, where the Brunauer-Emmett-Teller (BET) method and Barrett-Joyner-Halenda (BJH) model were employed to analyse surface area and pore size distribution, respectively.

2.3 Deoxygenation performance

TMPTO deoxygenation was performed using a 250 mL three-neck reactor under a steady nitrogen atmosphere (250 mL/min), with gas flow precisely adjusted using a mass flow regulator. A mixture of 50 g TMPTO and 2.5 g catalyst was loaded into the flask, followed by N_2 purging for 5 min to remove air. The reaction was initiated under heating (350 °C) and stirring (300 rpm) using a thermostatic magnetic stirrer (SCZL 500 mL, Shanghai Li-Chen Technology Co.). After 2 h, the system was cooled to room temperature under N_2. The reaction products were transported by N_2 into a condensation setup, where they were collected for subsequent analysis. Liquid-phase compounds were characterized using gas chromatography–mass spectrometry (GC-MS, Agilent 7890A-5975) equipped with an RB-1 AA-001-12410 capillary column. The extent of deoxygenation and the hydrocarbon selectivity were quantified by calculating GC peak areas, assuming proportionality between signal area and component concentration via the area normalization method. The deoxygenation and selectivity ratio of product were calculated using the following Eq(1) and Eq(2):

$$\text{Deoxygenation performance (\%)} = \frac{Alkane\ peak\ area + Alkene\ peak\ area}{Total\ peak\ area} \times 100\ \% \tag{1}$$

$$\text{Jet fuel hydrocarbon selectivity (\%)} = \frac{Total\ hydrocarbon\ peak\ area\ in\ the\ C8{-}C16\ range}{Total\ peak\ area} \times 100\ \% \tag{2}$$

3. Results and Discussion

Figure 2 presents the morphology and surface elemental distribution of NiFe/TiO_2 (FSP). Figure 2a-c present the surface morphology of the catalyst at different magnification levels. The catalyst particles have a spherical agglomerate structure with non-uniform particle size. It can be observed that the surface consists of spherical nanoparticle agglomerates. NiFe/TiO_2 (FSP) demonstrates pronounced particle aggregation, which may be attributed to the metal salts in the precursor liquid rapidly decompose, evaporate and nucleate to form primary nanoparticles, leading to dense particle generation in a short time and possible collision and aggregation to form unevenly sized aggregates before they are fully dispersed (Liu et al., 2019). In Figure 2d-i, the EDS results reveal uniformly distributed Ni and Fe elements, indicating homogeneous dispersion of these metals within the spherical structure. Additional EDS mapping was performed for C to investigate potential soot deposition from the combustion process during synthesis (Figure 2e). The absence of detectable carbon element in the EDS spectrum confirms no surface carbon contamination, eliminating the potential interference from carbonaceous species. Ti mapping shows distinct and evenly distributed point patterns, demonstrating uniform Ti distribution throughout the spherical structure. These results collectively suggest that Ni and Fe species are uniformly incorporated within the TiO_2 matrix, potentially indicating effective integration of NiFe components into the TiO_2 framework.

The crystalline phase structure of NiFe/TiO_2 (FSP) using 0.5 mol/L tetrabutyl titanate solution also differs significantly from the commercial anatase TiO_2. For comparison, TiO_2 (FSP) was synthesized through FSP of 0.5 mol/L tetrabutyl titanate solution. As revealed by XRD patterns in Figure 3a, the TiO_2 (FSP) exhibits a mixed-phase structure containing both anatase and rutile phase, with distinct rutile diffraction peaks appearing at 27.36°, 35.96°, 41.12°, 54.25°, 56.51° and 68.97° (Xu et al., 2024). Notably, the NiFe/TiO_2 (FSP) catalyst demonstrates the formation of characteristic Fe_5TiO_5 (pseudobrookite) and $NiTiO_3$ (ilmenite) phases, indicating that metal doping facilitates the development of iron titanate and nickel titanate structures (Jiang et al., 2022). This phase evolution suggests that the incorporated Ni and Fe species chemically interact with the TiO_2 matrix to form distinct ternary oxide phases rather than remaining as simple surface deposits. The mixed-phase Fe_5TiO_5/$NiTiO_3$-TiO_2 system enhances deoxygenation through three ways. The heterointerfaces facilitate substrate adsorption by providing abundant active sites, while the dynamic redox behaviour of metal species (e.g., Fe^{3+}/Fe^{2+} and Ni^{2+}) enhances oxygen mobility and reaction kinetics. Furthermore, electronic structure modulation at these interfaces optimizes the binding strength of oxygenates, thereby improving catalytic performance.

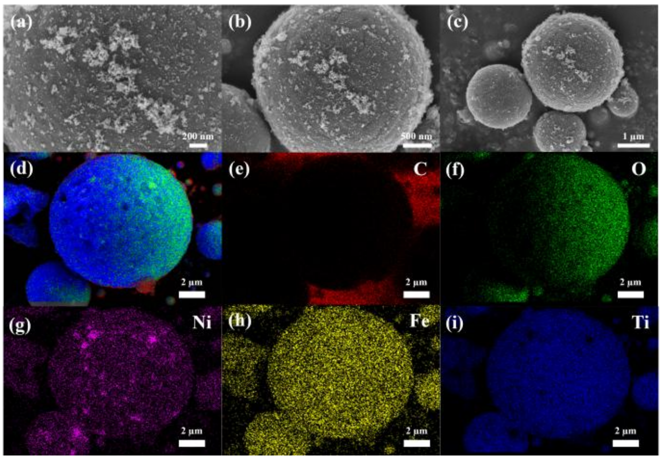

Figure 2: Morphology characterization of NiFe/TiO_2 (FSP) nanostructures: (a) 200 nm; (b) 500 nm; (c) 1 μm (d-i) EDS mapping of C, O, Ni, Fe, and Ti

The catalyst showed pore diameter 2.49 nm belonging to the mesopore range. In the Figure 3b. both catalysts exhibited typical type IV isotherms, confirming their mesoporous structures (Yang et al., 2014). NiFe/TiO_2 (FSP) possesses a specific surface area of 37.471 m²/g, a total pore volume of 0.059 cm³/g, and an average pore diameter of 3.072 nm, indicating that it is within the mesoporous regime. Despite its moderate surface area, the narrow pore diameter and substantial mesoporosity are expected to facilitate efficient molecular transport and active site exposure, both of which are beneficial for the deoxygenation reaction of biomass-derived intermediates. In comparison, sample A displayed a significantly higher adsorption capacity, but its hysteresis loop emerged only at $P/P_0 > 0.6$ and remained relatively narrow. This suggests the dominance of wider and less connected mesopores, potentially resulting from loose particle aggregation. Nevertheless, significant differences in pore structural regularity, specific surface area and hysteresis line morphology were observed, reflecting the profound influence of different preparation processes on the physical structure of the catalysts. These differences are attributed to the rapid quenching and high-temperature synthesis conditions inherent to FSP, which promote the formation of highly dispersed metal oxides and inhibit pore collapse. The NiFe/TiO_2 (FSP) catalysts exhibited moderate N_2 adsorption capacity and a broad hysteresis loop across the P/P_0 range of 0.2–0.8, indicating the presence of a complex, interconnected micro–mesoporous network. Although the surface area (37.471 m²/g) was lower than that of the WI sample, the extended hysteresis behavior suggests enhanced pore accessibility and potential for improved catalytic diffusion performance. Specifically, the well-developed mesoporous structure and high surface area of the FSP-derived catalyst promote efficient molecular diffusion and active site accessibility. This structure minimizes internal mass transfer resistance and ensures effective contact between reactants and active centers. As a result, it facilitates C-O bond cleavage and carboxylate group removal more efficiently under H_2-free conditions.

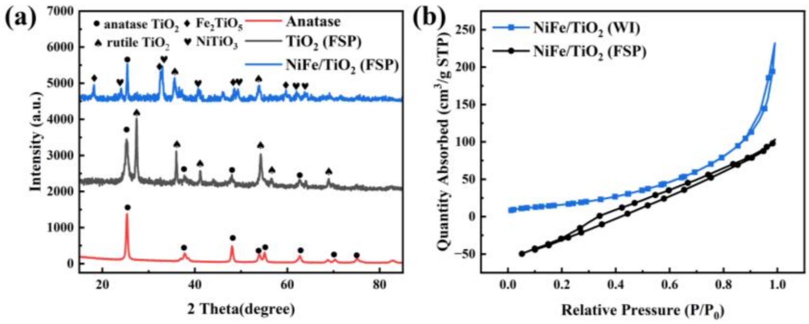

Figure 3: (a) XRD patterns of anatase TiO_2, TiO_2 (FSP) and NiFe/TiO_2 (FSP); (b) BET surface area analysis of NiFe/TiO_2

In Figure 4a, the NiFe/TiO_2 (FSP) catalyst exhibits significantly different product distributions compared to the NiFe/TiO_2 (WI). The total oxygenates content for NiFe/TiO_2 (WI) is 13.70 wt.% compared to 12.26 wt.% for NiFe/TiO_2 (FSP). Furthermore, NiFe/TiO_2 (FSP) produces a higher alkene yield of 47.14 wt.% compared to 42.87 wt. % for NiFe/TiO_2 (WI), while both catalysts maintain comparable alkane yields in the range of 40 % to 42 %. This shift suggests that the unique Fe_5TiO_5/$NiTiO_3$-TiO_2 heterostructure formed during FSP preferentially facilitates β-H elimination pathways under hydrogen-deficient conditions (Sun et al., 2025). With reduced "other" product and near-complete ester conversion, the NiFe/TiO_2 achieves efficient cascade deoxygenation through sequential decarbonylation/decarboxylation and subsequent C-C coupling (Cao et al., 2022).

As shown in Figure 4b, NiFe/TiO_2 (FSP) exhibited a slightly higher deoxygenation (conversion) rate of 87.49 %, compared to 85.31 % achieved by the NiFe/TiO_2 (WI). More notably, the NiFe/TiO_2 (FSP) demonstrated a significantly enhanced product (alkane and alkene) selectivity of 76.36 %, surpassing the 65.74 % selectivity observed in the NiFe/TiO_2 (WI). This improvement can be attributed to the superior metal dispersion and more uniform active site distribution for the FSP process, which promotes a more efficient cleavage of C-O bonds while suppressing side reactions. These results suggest that the FSP method not only facilitates higher deoxygenation efficiency but also favors the generation of targeted hydrocarbon products, making it a more effective strategy for bio-jet fuel production under mild, non-hydrogen conditions (Misra et al., 2023). The NiFe/TiO_2 (FSP) yields 24.11 wt.% cyclic products, indicating a stronger ability to promote carbon rearrangement, endocyclization, and aromatization of alkene intermediates-substantially outperforming the NiFe/TiO_2 (WI). (Pan et al., 2018).

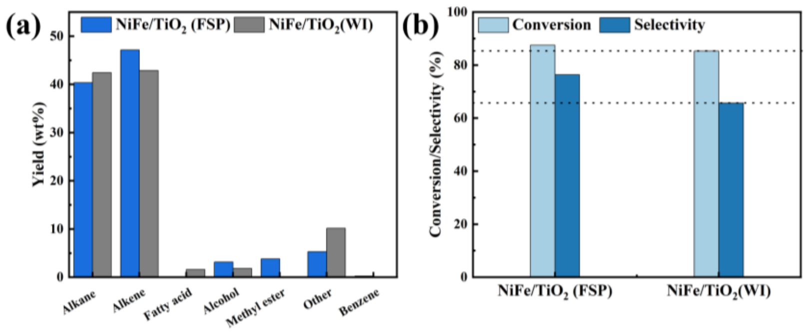

Figure 4: (a) deoxygenation yield of NiFe/TiO2 (FSP) catalysts prepared by wet-chemical and FSP methods; (b) conversion and selectivity of NiFe/TiO2 (WI) and NiFe/TiO2 (FSP)

4. Conclusions

In this study, FSP was demonstrated as an effective strategy to fabricate high-performance NiFe/TiO_2 (FSP) deoxygenation catalysts under N_2 atmosphere. FSP method enables rapid NiFe loading on TiO_2, which facilitates the synthesis of bifunctional catalysts. FSP-synthesized catalysts feature spherical structures formed by stacked nanoparticles, creating a porous network. Compared to dense aggregates from WI method, FSP catalysts offer higher surface area and more uniform porosity. This structure improves reactant diffusion and metal site exposure, enhancing deoxygenation and cracking. As a result, NiFe/TiO_2 (FSP) achieved 87.49 % deoxygenation efficiency in a N_2 atmosphere. This work highlights the potential of FSP in designing bimetallic catalysts for sustainable biojet fuel production under mild, H_2-free conditions.

Acknowledgments

The authors would like to thank The Research Fund for International Excellent Young Scientists (52250610220) awarded by the National Natural Science Foundation of China (NSFC).

References

Çakan A., Kiren B., Ayas N., 2023, Hydrodeoxygenation of safflower oil over cobalt-doped metal oxide catalysts for bio-aviation fuel production, Molecular Catalysis, 546, 113219.

Cao X., Zhao J., Long F., Liu P., Jiang X., Zhang X., Xu J., Jiang J., 2022, Efficient low-temperature hydrogenation of fatty acids to fatty alcohols and alkanes on a Ni-Re bimetallic catalyst: The crucial role of NiRe alloys, Applied Catalysis B: Environmental, 312, 121437.

Goh B.H.H., Chong C.T., Milano J., Tiong S.K., Cui Y., Ng J.-H., 2024, Response optimisation of TiO_2-supported bimetallic NiCo catalyst for the cracking and deoxygenation of waste cooking oil into jet-fuel range hydrocarbon fuels under non-hydrogen environment, Energy, 309, 133057.

Hartati H., Firda P.B.D., Prasetyoko D., Anggoro D.D., Bahruji H., Sakti S.C.W., Holilah H., Nugraha R.E., 2025, Conversion of volcano mud and marble waste to Ni/Ca/ZSM-5 catalyst for bio-jet fuel production from waste cooking oil and the effect of Ni loading, Fuel, 400, 135756.

Jiang F., Yin L., Feng G., Zhao Q., Yu Y., Hu Q., Zhang Q., Zhang X., Jiang W., 2022, Titanium Source Choice Affects the Nonhydrolytic Sol-Gel Synthesis and Morphology of Fe_2TiO_5, Chemistryselect, 7(13), e202104066.

Lei S., Zhang Y., Fang Z., Jin X., Li S., 2025, Spray flame synthesis of Y_2O_3/Al_2O_3 composite nanoparticles: Effects of precursor volatility and Y/Al ratio on particle morphology and crystal phase, Journal of Aerosol Science, 187, 106584.

Liu C., Pokhrel S., Tessarek C., Li H., Schowalter M., Rosenauer A., Eickhoff M., Li S., Mädler L., 2019, Rare-Earth-Doped $Y_4Al_2O_9$ Nanoparticles for Stable Light-Converting Phosphors, Acs Applied Nano Materials, 3(1), 699-710.

Minegishi N., Li P., Nagasawa T., Kosaka H., 2024, Effect of flame temperature on structure and CO oxidation properties of Pt/CeO_2 catalyst by flame-assisted spray pyrolysis, Applications in Energy and Combustion Science, 20, 100303.

Misra P., Alvarez-Majmutov A., Chen J., 2023, Isomerization catalysts and technologies for biorefining: Opportunities for producing sustainable aviation fuels, Fuel, 351, 128994.

Pan Z., Wang R., Chen J., 2018, Deoxygenation of methyl laurate as a model compound on Ni-Zn alloy and intermetallic compound catalysts: Geometric and electronic effects of oxophilic Zn, Applied Catalysis B: Environmental, 224, 88-100.

Romero M.A., Mayorga M.A., Gomez Z.E., Correa-Mahecha F., Suarez L.A., 2025, Life Cycle Assessment (LCA) of the Production of Sustainable Aviation Fuels (SAF) in Colombia, Chemical Engineering Transactions, 117, 343-348.

Sun S., Sun S., Zi W., 2025, Palladium-catalyzed enantioselective beta-hydride elimination for the construction of remote stereocenters, Nature Communications, 16(1), 2227.

Tang H., Dai Q., Cao Y., Li J., Wei X., Jibran K., Wang S., 2023, Production of jet fuel range hydrocarbons using a magnetic Ni-Fe/SAPO-11 catalyst for solvent-free hydrodeoxygenation of jatropha oil, Biomass and Bioenergy, 177, 106927.

Wei K., Feng X., Jiang H., 2024, Improvement of heat resistance in silicone rubber by Fe-doped TiO_2 nanoparticles prepared via flame spray pyrolysis, European Polymer Journal, 214, 113139.

Wu P., Cai C., 2022, Supported Pt-Ni bimetallic nanoparticles catalyzed hydrodeoxygenation of dibenzofuran with high selectivity to bicyclohexane. Chinese Chemical Letters, 33(1), 234-238.

Xu C., Long Q., Zhong S., Wang W., Guo J., Yang J., Wang X., Dai L., 2024, Insights into the Synergistic Catalytic Effect of TiO_2 Supported V-W Oxides for Selective C−H Bond Oxidation of Cyclohexane to KA Oil, Chemistry – A European Journal, 30(70) e202402780.

Yang Y., Ochoa-Hernández C., de la Peña O'Shea V.A., Pizarro P., Coronado J.M., Serrano D.P., 2014, Effect of metal–support interaction on the selective hydrodeoxygenation of anisole to aromatics over Ni-based catalysts, Applied Catalysis B: Environmental, 145, 91-100.

Zhang H., Goh B.H.H., Chong C.T., Zhang Y., Lee C.T., Gao Y., Tian B., Tran M.-V., Mohd Yasin M.F., Ng J.-H., 2024a, A review of flame aerosol synthesis technology for the synthesis of nanoparticles and functional energy materials, Journal of Solid State Chemistry, 336, 124774.

Zhang J., Goh B.H.H., Ng J.-H., Chong C.T., 2024b, Upgrading of Trimethylolpropane Oleate to Biojet Fuel Range Hydrocarbons Through Catalytic Deoxygenation, Chemical Engineering Transactions, 112, 277.